A Lidar Approach to Measure CO_2 Concentrations from Space for the ASCENDS Mission

James B. Abshire[1], Haris Riris[1], Graham R. Allan[2], Clark J. Weaver[3], Jianping Mao[3], Xiaoli Sun[1], William E. Hasselbrack[2], Anthony Yu[3], Axel Amediek[4], Yonghoon Choi[5], Edward V. Browell[5]

[1] *NASA Goddard Space Flight Center, Greenbelt, MD 20771, USA*
[2] *Sigma Space Inc., Lanham, MD 20706 USA*
[3] *Goddard Earth Sciences and Technology Center, UMBC, Baltimore, MD 21228, USA*
[4] *Deutsches Zentrum fuür Luft- und Raumfahrt (DLR), 82234 Wessling, Germany*
[5] *NASA Langley Research Center, Hampton VA 23681, USA*

Keywords: Space lidar, CO_2, Airborne lidar, Differential Absorption Lidar

ABSTRACT

We report on a lidar approach to measure atmospheric CO_2 column concentration being developed as a candidate for NASA's ASCENDS mission. It uses a pulsed dual-wavelength lidar measurement based on the integrated path differential absorption (IPDA) technique. We demonstrated the approach using the CO_2 measurement from aircraft in July and August 2009 over various locations. The results show clear CO_2 line shape and absorption signals, which follow the expected changes with aircraft altitude from 3 to 13 km. The column absorption measurements show altitude dependence in good agreement with column number density estimates calculated from airborne in-situ measurements. The approaches for O_2 measurements and for scaling the technique to space are discussed.

1. INTRODUCTION

Although increasing atmospheric CO_2 is widely accepted as the largest anthropogenic factor causing climate change, there is considerable uncertainty about its global budget. Accurate measurements of tropospheric CO_2 mixing ratios are needed to study CO_2 emissions and CO_2 exchange with the land and oceans. To be useful in reducing uncertainties about carbon sources and sinks the atmospheric CO_2 measurements need deg-level spatial resolution and ~ 0.3% precision [1,2]. Several groups have analyzed the potential of space missions using passive spectrometers [3-5], and the GOSAT mission [6] is now making global CO_2 measurements from space using an FTIR spectrometer and surface reflected sunlight. However sun angle limitations restrict its measurements to the daytime and mid-latitudes. An inherent error source with space-based passive spectrometers is optical scattering from thin clouds, particularly cirrus, in the measurement path [7,8]. Optical scattering in the measurement path modifies the optical path length and thus the total CO_2 absorption viewed by passive spectrometers. It can cause large retrieval errors even for thin cirrus clouds [9].

To address these limitations, the US National Research Council's 2007 Decadal Survey for Earth Science recommended a new space-based CO_2 measuring mission called ASCENDS [10]. Its goals are to produce global atmospheric CO_2 measurements using the laser absorption spectroscopy measurement approach. The mission's goals are to quantify global spatial distribution of atmospheric CO_2 with 1-2 ppm accuracy, and quantify the global spatial distribution of terrestrial and oceanic sources and sinks of CO_2 on 1-degree grids with approximately monthly time resolution. The ASCENDS approach offers continuous measurements over the cloud-free oceans, at low sun angles and in darkness, which are major advantages over passive sensors. ASCENDS mission organizers held a workshop in 2008 to better define the science and measurement needs and planning for future work [11]. ESA has also conducted mission definition studies for a similar space mission called A-SCOPE [12,13]. The lidar sensitivity and spectroscopic analyses performed as part of the A-SCOPE definition activities have been recently published [14,15].

2. LIDAR APPROACH

Several groups have measured atmospheric CO_2 absorption using DIAL lidar techniques. A summary of these has been recently published [16]. Our group has been developing a pulsed lidar approach as a candidate for the

Lidar Technologies, Techniques, and Measurements for Atmospheric Remote Sensing VI,
edited by Upendra N. Singh, Gelsomina Pappalardo, Proc. of SPIE Vol. 7832, 78320D
 · doi: 10.1117/12.868567

ASCENDS mission [17-19]. The approach, shown in Figure 1, uses a dual band pulsed laser absorption spectrometer and the integrated path differential absorption (IPDA) lidar technique. The approach uses two tunable pulsed laser transmitters allowing simultaneous measurement of the absorption from a CO_2 absorption line in the 1570 nm band, O_2 extinction in the oxygen A-band, and surface height and atmospheric backscatter in the same path. A tunable laser is stepped in wavelength across a single CO_2 line for the CO_2 column measurement, while simultaneously a laser is stepped across a line doublet near 765 nm in the Oxygen A-band for an atmospheric pressure measurement [20, 21]. Both lasers are pulsed at a ~8kHz rate, and the two absorption line regions are sampled in wavelength steps at typically ~1 KHz. Both laser transmitters utilize tunable diode lasers followed by laser amplifiers. The direct detection receiver measures the time resolved laser backscatter from the atmosphere along with the energies of the laser echoes from the surface. After suitable averaging the gas extinction and column densities for the CO_2 and O_2 gases are estimated from the sampled wavelengths of the surface reflected line shapes via the Differential Absorption Lidar (DIAL) technique [22].

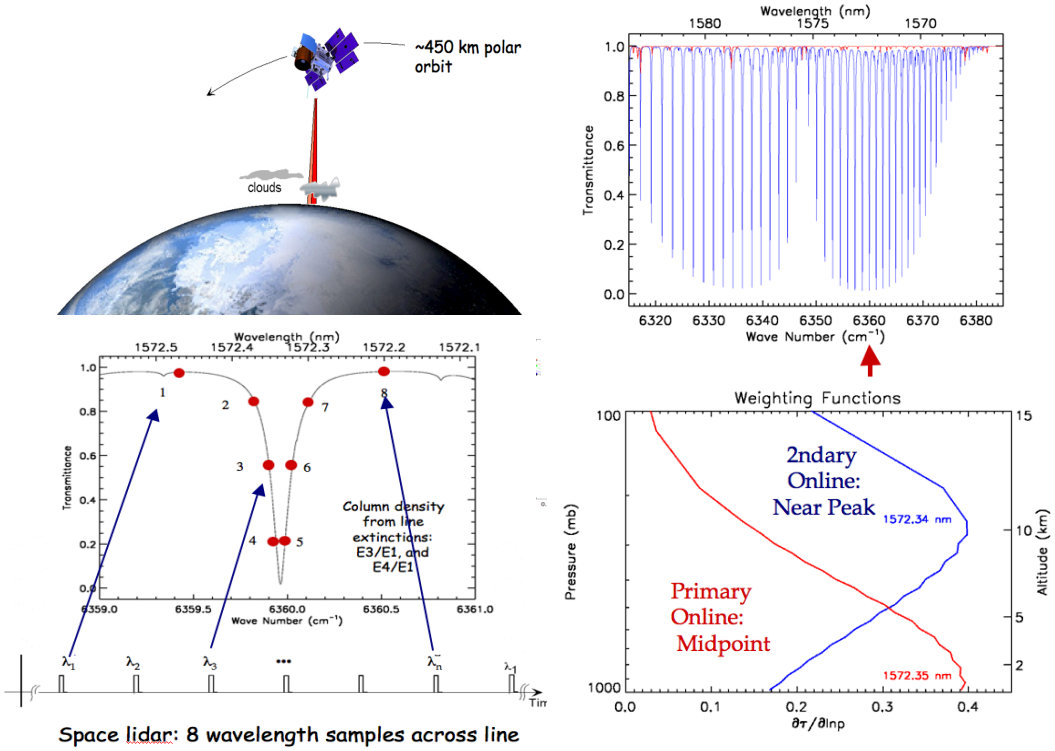

Figure 1 – *Top Left* – Space measurement concept. *Top right* - 2-way transmission for the 1570 nm CO_2 band from space computed from HITRAN 2004. The technique measures the absorption of a single line in this band. *Bottom Left*- The present selection of the 1572.33 nm CO_2 line, and wavelength sampling strategy for space. *Bottom Right* – The computed weighting functions for the space measurement using the ratio of the mid-point wavelengths (points 3 and 6) to offline ratio (in red) and the near peak (points 4 and 5) to offline ratio (in blue). The red curve shows the nearly uniform tropospheric vertical weighting function which is needed for the ASCENDS flux determinations.

The approach is flexible, and the concept for space measures the CO_2 lineshape at 8 wavelengths. This provides several capabilities and allows using vertical atmospheric weighting functions at 2 heights [23]. Sampling at multiple wavelengths across the absorption line allows for solving for wavelength offsets via a line fitting process. The distributed wavelength sampling across the line region also allows the instrument's response to be characterized as a function of wavelength. These capabilities allow modeling and reducing the impacts of wavelength dependent responses in the lidar. Using pulsed lasers and receiver processing to time (and height) resolve the laser backscatter profiles also allows post detection signal processing to isolate the laser echo signals from the surface, and to reject laser photons scattered from the atmosphere which arrive earlier. Hence it allows isolating the full column measurement from bias errors caused by atmospheric scattering [7,8]. Isolating the surface echo with a time gate in

receiver processing also substantially improves the receiver's signal-to-noise ratio by reducing the amount of noise from the detector and the solar background.

3. CO_2 SPECTROSCOPY AND LINE CHOICE

We use a single line in the 1570 nm band (Fig. 1) for the CO_2 measurement [7]. This vibration-rotation band of CO_2 has an appropriate range of absorption that provides good sensitivity to the surface echo signal and to variation in CO_2 in the lower troposphere. This band has minimal interference from other atmospheric species like H_2O, and has several different temperature insensitive lines. The shorter wavelength lines in the R-branch are a better match to available laser and detector technologies. The centermost line of R-branch at 1572.335 nm, shown in Figure 1, has been analyzed and appears as an attractive line for CO_2 measurements [23]. It has the minimum temperature sensitivity, particularly to the lower atmospheric temperature changes. It also provides the maximum CO_2 absorption in the R-branch. Absorption measurements on this line at different wavelengths yield the line shape and CO_2 vertical column densities with weighting functions peaking at different altitudes.

4. PULSED IPDA MEASUREMENT APPROACH

The IPDA technique is a well-established lidar technique for open-path laser absorption spectroscopy measurements [22,24]. It is essentially a special case of differential absorption lidar, where a scattering target (such as the ground, a water surface, or cloud tops) is used at the end of the path. Typically two laser wavelengths are used, and the target is illuminated with the laser alternatively tuned onto the gas absorption line, and off it. The path-integrated gas absorption attenuates the on-line laser energy relative to the off-line wavelength. By measuring the optical depth of the gas absorption line and range, and by knowing the difference in gas absorption cross-sections, one can solve for the path integrated gas number density. In our lidar the photon counting receiver records and accumulates the time resolved backscattered photon counting profiles for the wavelength steps across the line for a given integration time. This allows recording the cumulative laser backscatter profile at each transmitted wavelength. This contain time resolved atmospheric backscatter as well as the surface echo pulses at each wavelength. The absorption line shape and optical depth are computed from the echo pulse energies, usually at the longest range at the end of the path.

The error of the lidar measurement of optical depth and path integrated number density depends on its signal and noise characteristics and the magnitude of bias errors. A detailed analysis must account for many factors, including variability in the lidar parameters, atmospheric temperature and pressure, turbulence, laser speckle, changing surface reflectivity and range, etc. [14,15]. A simplified treatment for this approach, for an open atmospheric path and target at a fixed range R, illustrates most of the important dependencies, and is given in [16].

5. AIRBORNE LIDAR DESCRIPTION

In 2007, we demonstrated ground-based lidar [25] measurements of column CO_2 absorption in horizontal paths. In 2008 we adapted the lidar for use on the NASA Glenn Lear-25 aircraft [26] shown in Figure 2. A block diagram of the flight instrument is shown in Figure 3. Modifications to the ground-based lidar included converting the laser transmitter to pulsed operation by adding an acousto-optic modulator (AOM) between the diode laser and the fiber amplifier, removing the chopper wheel, and improving the receiver sensitivity by using a PMT detector, followed by a discriminator and multi-channel scaler (MCS). The airborne lidar specifications are listed in Table 1.

Figure 2- *Left* - NASA Glenn Lear-25 aircraft. The nadir window assembly is just below the NASA logo. Photographs of the lidar installed on the aircraft showing the sensor head assembly *(Middle)* and the dual aircraft racks *(Right)*.

Table 1 – 2009 Pulsed Airborne CO_2 Lidar Parameters

CO2 line center wavelength	1572.33 nm (typically)		Telescope diameter	20 cm
Laser min & max wavelengths	1572.29 nm, 1572.39 nm		Receiver FOV diameter	200 µrad
Laser wavelength steps across line	20 (these flights)		Receiver optical bandwidth	800 pm FWHM
Laser wavelength change/step	~ 5 pm		Receiver Optics Transmission	64%
Laser peak power, pulse width, energy	25 watts, 1 µsec, 25 µJ		Detector PMT type	Hamamatsu H10330A-75
Laser divergence angle	100 µrad (these flights)		Detector quantum efficiency	2% (this device)
Seed laser diode type	DFB: Fitel FOL15DCWD		Detector dark count rate	~ 500 kHz
Laser Pulse Modulator (AOM)	NEOS Model: 26035-2-155		Receiver signal processing	Photon counting/histogramming
Fiber coupled CO2 cell	80 cm path, ~200 Torr pressure		Histogram time bin width	8 nsec
Fiber Laser Amplifier (EDFA)	IPG EAR-10K-1571-LP-SF		Receiver integration time	1 second per readout
Laser line scan rate	450 Hz		Recording duty cycle	50% (1 sec. every 2 sec.)
Laser linewidth per step	~15 MHz		Instrument rack size & mass:	~ 90 cm tall, total: 147 kg
Receiver Telescope type	Cassegrain, f/10 (Vixen)		Sensor head size and mass	~ 25 x 60 x 60 cm, 41 kg

A laser signal drawing and lidar block diagram are shown in Figure 3. The lidar signal source is a DFB laser diode, which is operated near 1572.33 nm by controlling its temperature and current. A ramp from a signal generator was used to sweep the current to the diode laser, and hence its output wavelength. The diode's CW output is then gated into pulses using an acousto-optic modulator (AOM) to an Erbium Doped Fiber Amplifier (EDFA). A small percentage of the CW seed laser output is split off and directed through a fiber-coupled CO_2 absorption cell and to a PIN detector. The CO_2 cell serves as a monitor for center wavelength of the sweep. The nominal static transmitted laser pulse wavelengths are measured in a calibration procedure using a commercial wavemeter . Subsequent testing showed some curvature in the scanning dynamic ramp signal, so we used a more accurate quadratic functional model for the laser wavelength vs pulse position in the data analysis.

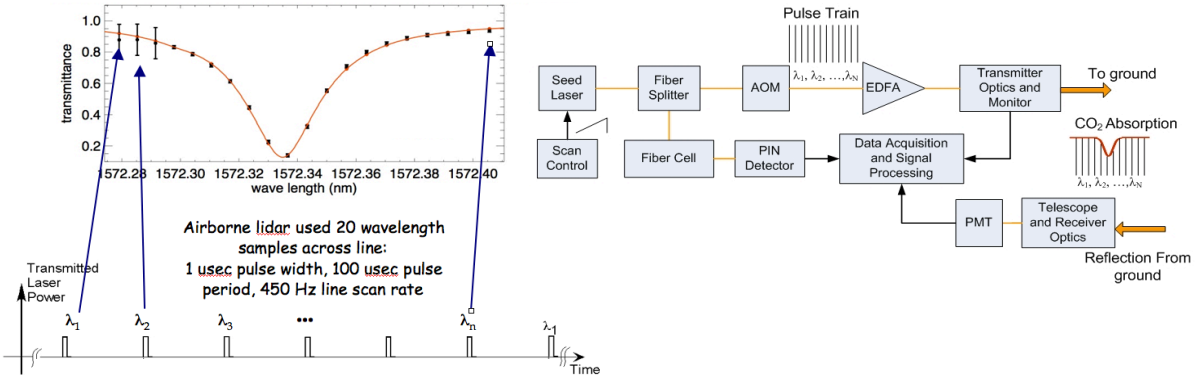

Figure 3. *Left* – CO_2 Line sampling approach for airborne lidar. *Right* – CO_2 lidar channel block diagram.

The laser output is a sequence of 1usec-wide laser pulses, shown in Figure 4, which occur at a 10 KHz rate. A sample of the laser diode sweep through the internal cell containing CO_2 is shown with a sample of the pulsed transmitter wavelength sweep, along with the optical power vs time waveform of a single pulse from the transmitter. The collimated transmitted laser signal exits through nadir aircraft window. The laser backscatter is collected by the receiver's 20 cm diameter Cassegrain telescope, which views nadir through the same window in a bistatic configuration. A multimode fiber is used to couple the optical signal from the telescope focal plane to the receiver optics. After passing through an optical bandpass filter, the signal is focused onto a PMT detector. The PMT used in the 2009 flights had a single photon counting efficiency of ~2%. The electrical pulse output from the PMT was amplified and passed through a threshold detector.

The pulses from the receiver's PMT detector and discriminator are binned and accumulated by the MCS. The start time of the MCS sweep is synchronized with the first laser pulse trigger and hence start of the pulsed wavelength sweep. Each MCS sweep contains a histogram of PMT pulse counts vs time for the wavelength sweeps (i.e. the laser backscatter profiles for all 20 pulses). At the end of 1 second, each bin contains the total receiver counts for the 450 laser sweeps. The receiver histogram record is then read and stored. The laser trigger and data acquisition is synchronized to timing markers from the GPS receiver and data was stored every other second. The computer also

digitizes other signals, including those from thermocouples distributed across the sensor head and electronic rack, the inertial guidance system output from the aircraft and GPS position and time. A nadir viewing video camera also records the visible image though the window.

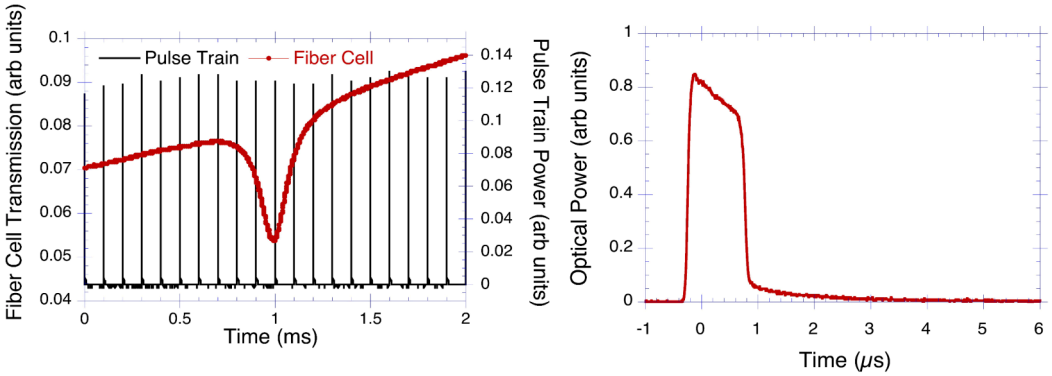

Figures 4. *Left* – Example of the laser wavelength scan. (red trace and left hand axis) - Sample cw wavelength scan of the diode laser (before the modulator) through the instrument's internal pressure CO_2 cell, showing CO_2 absorption and diode laser power variability vs wavelength. (Black trace and right hand axis) – Detected laser output power vs time from the laser transmitter's power monitor. *Right* - Typical single laser pulse (in red, left hand axis) from the airborne laser transmitter. The pulse shape shows decay as the fiber amplifier gain is depleted. The 1usec wide part of the laser pulse contains over 90 % of the pulse energy.

7. 2009 AIRBORNE CAMPAIGNS

We used the NASA Glenn Lear-25 aircraft [26] for these flights. The airborne lidar is configured into two half-racks and a "sensor head", which contained the receiver telescope and the transmitter optics. A photograph of the sensor when integrated on the aircraft is shown in Figure 2. The sensor head was mounted above the aircraft's nadir viewing window. For the 2009 flights a pair of wedged and anti-reflection coated optical windows were used in the aircraft's nadir window assembly.

During late-July though mid-August 2009 we flew an airborne campaign with a series of 2.5 hour-long flights. We measured the shapes of the atmospheric CO_2 absorption line at stepped altitudes from 3-13 km over a variety of surfaces in Nebraska, Illinois, the SGP ARM site, and near and over the Chesapeake Bay in North Carolina and eastern Virginia. Strong laser signals and clear CO_2 line shapes were observed at all altitudes on most flights, and some measurements were made through thin and broken clouds. These flights allowed testing and recording performance under different measurement conditions. These included measuring to the ground through broken and thin clouds. An example of these measurements is shown in Figure 5.

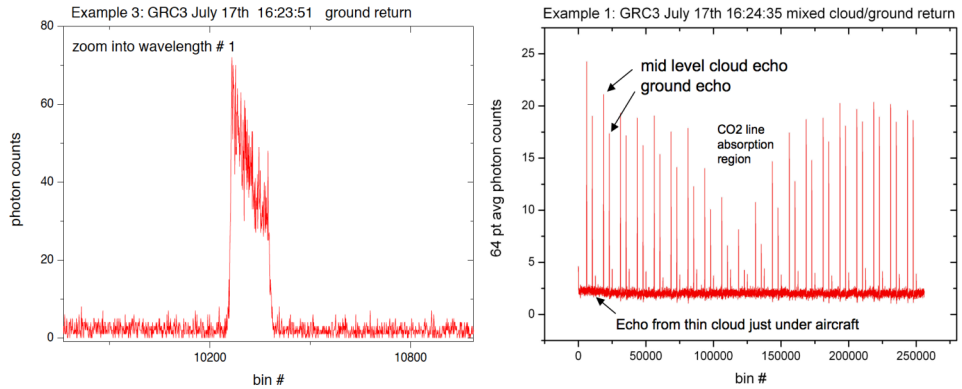

Figure 5. *Left* - A typical single accumulated pulse shape measured from the ground echoes from the photon counting receiver. *Right* - Example of a raw (uncorrected) recorded backscatter profile when measuring to the ground through 2 thin cloud layers. It shows 3 time displaced echo pulses per transmitted pulse. The smallest initial echo pulses are from the cirrus clouds just under the aircraft. The figure also shows the two range displaced CO_2 column absorptions which are evident in the echoes from the mid-level cloud layer and the deepest absorption in the longest path to the ground.

The figure shows the time resolved triple-echo pulses measured when viewing the ground over Ohio through two thin clouds layers. The first pulse in each triplet is the reflection from the cirrus cloud, while the second is reflection from the mid altitude cloud and the third from the ground. The different amounts of CO_2 column absorption for the different path lengths are evident. Without a range resolved receiver, the echo pulse signals and measurements from the three different path lengths would be mixed. Using the pulsed measurement approach allows using range gating in the data processing to isolate the signals from the surface and hence eliminates optical path length errors from atmospheric scattering.

8. AIRBORNE CO_2 MEASUREMENTS AND CALCULATIONS

In order to estimate the actual CO_2 column density during the flights, measurements of atmospheric temperature, moisture and pressure vertical profiles were used from the radiosonde balloons, which were launched near the flight location. Their parameters were used in a 40 layer atmospheric model to compute dry air column density vs height to 13 km altitude. The airborne flights were also coordinated with LaRC investigators, and the flights over the ARM site, NC and VA were under-flown with in-situ gas measurements made from the NASA LaRC UC-12 aircraft. This used a quick-response infrared absorption gas analyzer to measure CO_2 concentrations. It sampled air and CO_2 concentrations every second from takeoff to the aircraft's upper flight altitude and back to the ground.

The AVOCET (Atmospheric Vertical Observation of CO_2 in the Earth's Troposphere) *in-situ* CO_2 measurement system [28,29] was used to obtain high-precision, high-accuracy measurements of CO_2 mixing ratios profiles under the flight track of the GSFC CO_2 Sounder during the flights over Oklahoma, North Carolina and Virginia. AVOCET uses a modified LI-COR model 6252 non-dispersive infrared (NDIR) gas analyzer-based sampling system with dual sample cells to achieve high CO_2 measurement precision by comparing the differential absorption between the sampled air and a calibrated reference gas that is traceable to the World Meteorological Organization primary calibration standards maintained at the National Oceanic and Atmospheric Administration, Climate Monitoring and Diagnostics Laboratory in Boulder, Colorado. During ambient sampling, air was continuously drawn through a Rosemount probe, a permeable membrane dryer to remove $H_2O_{(v)}$, the LI-COR analyzer, and then through the diaphragm pump. Frequent but short calibrations with well-documented and stable calibration gases, critical to achieving both high precision and accuracy, were accomplished by periodically (~15 minutes) flowing calibration gas through the instrument's sample cell. The system was operated at a constant mass flow rate (500 cm^3 min^{-1}) and pressure (250 torr), and had a CO_2 measurement precision of ≤ 0.1 ppm ($\pm 1\sigma$) and accuracy of ±0.25 ppm for 1 Hz sampling rates. AVOCET CO_2 measurements were made from a maximum altitude of 8 km to below 300 m AGL (above ground level). In the case, when the spiral was done over a "low-use" airport, the *in situ* measurements were done down to the ground in a "touch and go" of the airport runway. All AVOCET measurements were integrated with GPS latitude, longitude, and altitude measurements made on the UC-12. The spirals were timed to coincide with over-flights of the GSFC CO_2 sounder. The line shape, averaged 2-way optical depth for the 1572.335 nm line, and the CO_2 column number density were computed versus flight altitude based on these readings. These calculations provided a reference comparison for the airborne lidar measurements and showed how the CO_2 line shapes and depths should vary with flight altitude.

Vaisala RS-92 radiosondes were also launched during each test flight to obtain the meteorological parameters needed for converting the CO_2 mixing ratios measured by AVOCET to the path integrated CO_2 column density needed to compare with the lidar. The RS-92 radiosondes have a pressure, temperature, and relative humidity absolute accuracies from 1080-100 hPa of 1 hPa, 0.5 ^oC, and 5%, respectively. These radiosondes were launched from the ground at the center of the UC-12 spiral location, and when possible, they were launched at the completion of the UC-12 spiral. Close coordination was maintained between the UC-12, Lear-25, and ground radiosonde personnel to ensure the most coincident data acquisition for comparison of the remote and in situ-derived CO_2 data.

9. 2009 CO_2 MEASUREMENT PROCESSING

For the flights the lidar recorded the time- and wavelength-resolved laser backscatter with 1second integration time. In subsequent analysis, the line shape measurements at each flight altitude step where averaged. We used a CO_2 line retrieval approach based on the Gauss-Newton method [30] to analyze each altitude averaged line shape. This approach has sufficient free parameters to model and correct for instrument effects, to fit the resulting CO_2 line shapes, and to estimate the corresponding CO_2 column densities and optical depth at each altitude. The CO_2 retrieval

algorithm yields an estimate of the mean CO_2 column density over the laser path length based on line absorption strength taken from the HITRAN 2004 database. The input observations were the ratio of the photon counts in the surface echo signals at each wavelength after they were normalized by an estimate of transmitted pulse energy. The error covariance matrix for the observed signals was diagonal and equally weighted for all but the first three wavelengths. Examples of calculated and the observed (retrieved) line shapes for the 8/4/09 flight over the ARM site and the 8/17/09 flight over North Carolina are shown in Figures 6 and 7.

The algorithm requires several other inputs. First are estimates of the vertical profile of temperature, pressure and water vapor versus altitude. These are used to calculate the approximate CO_2 line shape, and were estimated from gridded meteorological fields from the Goddard Modeling and Assimilation Office for the locations at the time of the flights. They are used to calculate the wavelength resolved absorption spectra of atmospheric CO_2 based upon HITRAN 2004 for each 1 km altitude bin. The algorithm also uses the path length from the aircraft to the surface, which was calculated from the laser pulse's time of flight. Based on both ground-based testing and subsequent airborne measurements, the range resolution for these flights was estimated to be < 5m. Since this was ~0.2% or less of the column height, its contribution to the overall CO_2 measurement error was negligible.

The algorithm attempts to fit the sampled CO_2 line shape using a model with several sets of variables. The first is the reduction of the photon count ratio near the 1572.335 nm line due to CO_2 absorption. Since the photon counts for the line shape samples are measured as a function of pulse number, they are converted to wavelength before comparing the observed spectra with the HITRAN data. For these experiments the lidar's wavelength (ie wavelength per laser pulse number) was modeled as a quadratic function, and the three wavelength coefficients were solved for, using the ground calibration as a prior constraint. The final set of variables modeled the changes in the lidar's baseline response with wavelength. This product can change during flight due to the changing physical environment of the lidar. We fit (modeled) and normalized for an estimate of the baseline variability using a quadratic energy dependence with pulse number.

The CO_2 column results are being analyzed by flight location. The measured CO_2 column density vs altitude plots in Figures 6 and 7 were computed from the in-situ sensor readings from the LaRC aircraft (red line, lower x-axis). Other analysis of the 2009 flights showed that the average signal levels follow predicted values [31], and that the altimetry measurements over water had an uncertainty of ~3 m [32]. Although the CO_2 absorption analysis is continuing, the preliminary agreement on these flights between the estimated optical depths from the lidar, and the computed ones is quite good.

10. OXYGEN ABSORPTION MEASUREMENT

In order to accurately estimate the CO_2 mixing ratio, the ASCENDS mission requires a measurement of the dry air column density simultaneously with the CO_2 column. Our group is also developing a lidar approach to measure atmospheric pressure in the same path by adding a parallel lidar channel with measures column absorption of a line pair in the O_2 A-band [20, 21]. We have developed a breadboard lidar for O_2, and measured its column absorption from the laboratory over an outdoor horizontal path using the instrument shown in Figure 8. In July 2010 we demonstrated airborne measurements of O_2 column absorption using this approach. These results will be reported in the future.

11. SCALING TO SPACE

A space-based version of this lidar must have a much larger lidar power-area product due to the ~x40 longer range and faster along track velocity. We have developed receiver SNR models for both the CO_2 and O_2 channels and applied them to estimate lidar parameters needed for the space measurement. Some initial calculations used to estimate the needed laser energies for a space are shown in Figure 9. These are for a 500 km orbit, a 1.5 m diameter telescope and a 10 second integration time, which allows a 70 km along track integration in low earth orbit. The received SNR and relative measurement error are plotted versus laser peak power for a 1-usec wide laser pulse in Figure 9. The calculations show that ~3 mJ laser energies are required to attain the precision needed for each measurement. These calculations are conservative by 3 dB since they assume that only single on- and off-line measurements are made, where our approach uses twice as many measurements.

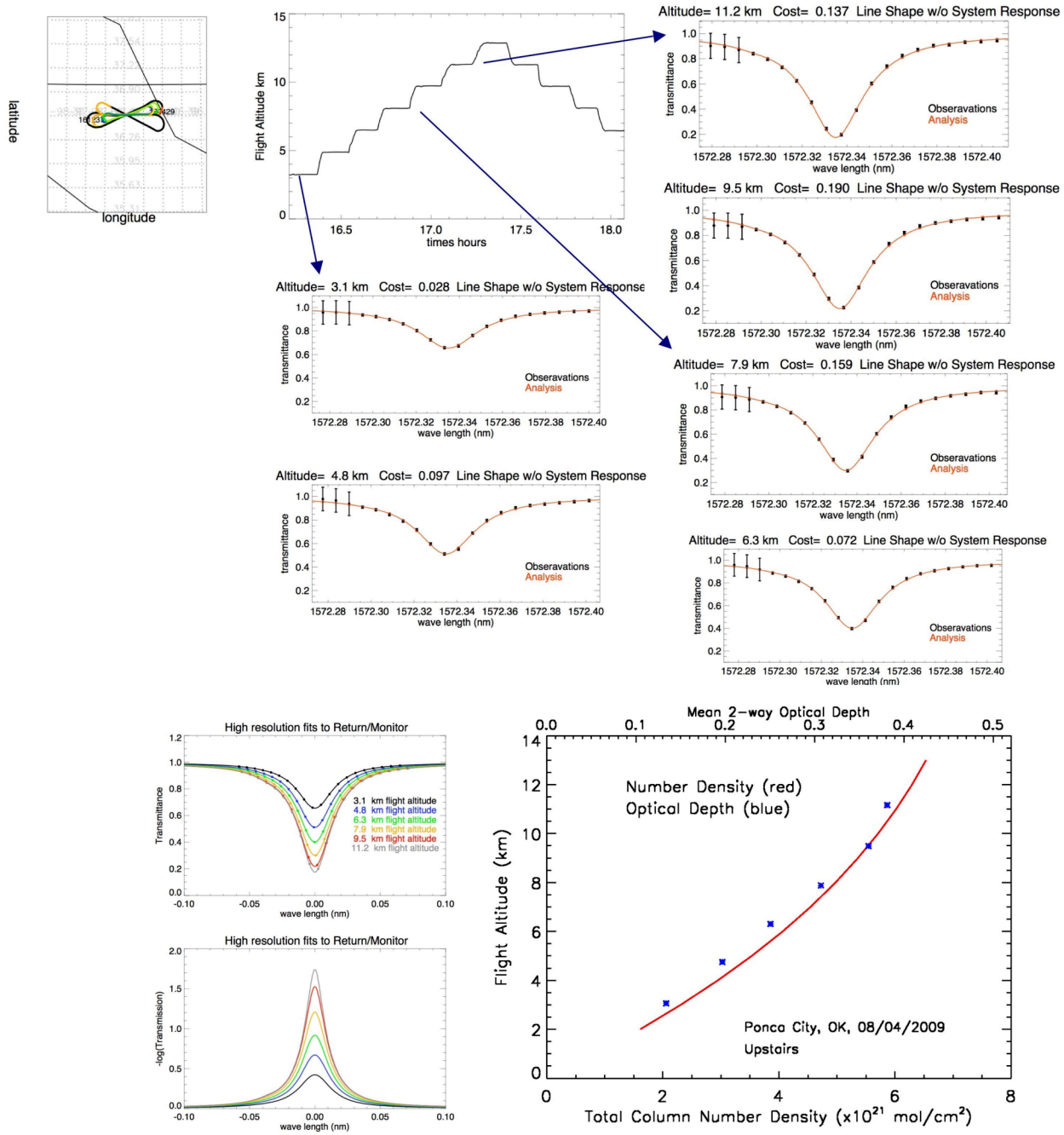

Figure 6- Top – *Top set* - Outline of the flight pattern and sample measurements of the 1572.33 nm CO_2 line for flight above the DOE SGP ARM site on 8/4/09. *Left* – map of location of "bowtie" flight patterns. The altitude changes in curved part of one bowtie, *Center top* – Altitude history of flight, showing aircraft altitude steps from 3.1 to 11.2 km, *Other upper plots* – measured CO_2 absorption line shapes (black dots) at the constant altitude steps given and orange lines showing CO_2 line shape fits through the measurements. *Bottom plots* - Initial analysis of the 1572.33 nm CO_2 shape measurements for this flight. – Overlayed plot of the fitted CO_2 line transmission vs wavelengths, from Figure 4, for the altitudes indicated. *Bottom Left* – Computed CO_2 optical depths vs wavelength from the optical transmissions. *Right*– plot of measured CO_2 absorption mean optical depths (in blue, for upper x-axis), vs altitude. The measured CO_2 column density vs altitude computed from the in-situ sensor readings from the LaRC aircraft (red line, for lower x-axis). There was a smooth increase in measured optical depth, except for the measurement at 9.5 km altitude.

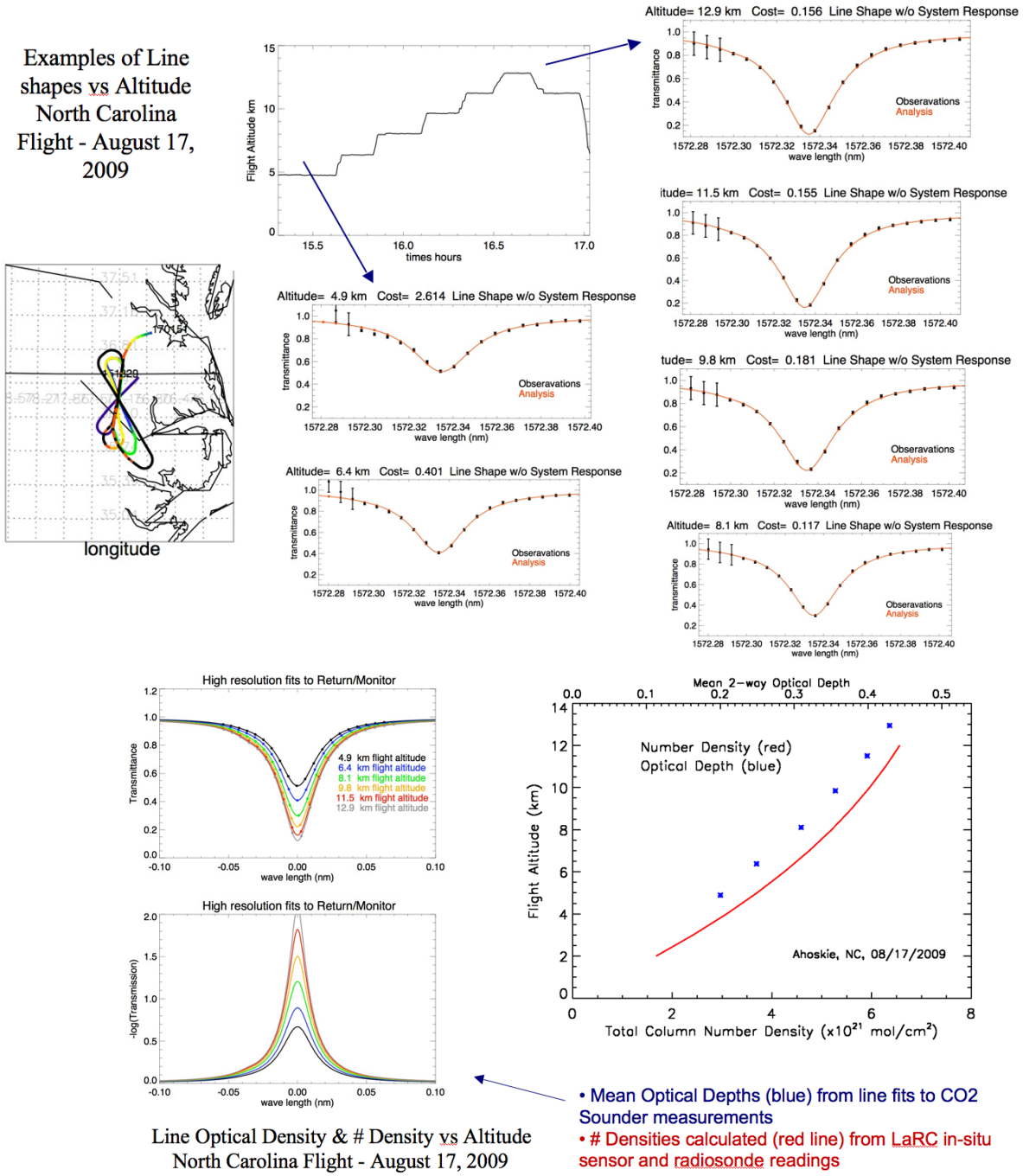

Figure 7- Top – *Top set* - Outline of the flight pattern and sample measurements of the 1572.33 nmCO_2 line for flight above North Carolina on 8/17/09. *Left* – map of location of "bowtie" flight patterns. The altitude changes in curved part of one bowtie, *Center top* – Altitude history of flight, showing aircraft altitude steps from 4.9 to 12.9 km, *Other upper plots* – measured CO_2 absorption line shapes (black dots) at the constant altitude steps given and orange lines showing CO_2 line shape fits through the measurements. *Bottom plots* - Initial analysis of the 1572.33 nm CO_2 shape measurements for this flight. – Overlayed plot of the fitted CO_2 line transmission vs wavelengths, from Figure 4, for the altitudes indicated. *Bottom Left* – Computed CO_2 optical depths vs wavelength from the optical transmissions. *Right*– plot of measured CO_2 absorption mean optical depths (in blue, for upper x-axis), vs altitude. The measured CO_2 column density vs altitude computed from the in-situ sensor readings from the LaRC aircraft (red line, for lower x-axis). There was a smooth increase in measured optical depths vs altitude, which matched the calculated trend.

Based on these SNR and laser energy estimates the Goddard Instrument Development Laboratory has conducted two space lidar design studies for ASCENDS. The instrument concept drawing from the first study is shown in Figure 9.

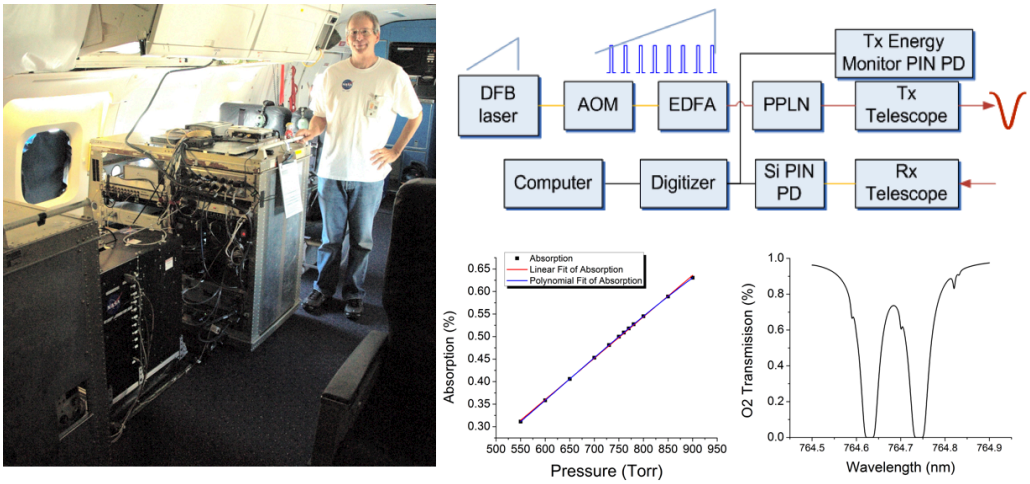

Figure 8- Oxygen lidar measurement channel. *Left*- Photograph of the combined CO_2 and O_2 lidar flown in July 2010 on the NASA DC-8 with Randy Kawa. – *Top right* – O_2 lidar channel block diagram, where the receiver telescope is shared with the CO_2 channel. Some parameters of the breadboard O2 lidar are: Diode laser wavelength: 1529-1530 nm, Laser amplifier: NP Photonics EDFA, Lidar measurement wavelength: 764.5 – 764.9 nm, Laser pulse energy: ~2 uJ/pulse, laser pulse width: 250 nsec, Laser pulse rate: 10 KHz Number of wavelength steps: 40, Detector type: Si APD (SPCM). *Bottom middle* – Calculation showing nearly linear dependence of the absorption of the valley between the two O_2 lines with surface pressure. *Bottom right* - Calculated absorption for the O_2 line doublet vs wavelength for a horizontal path with a target at 1.5 km range.

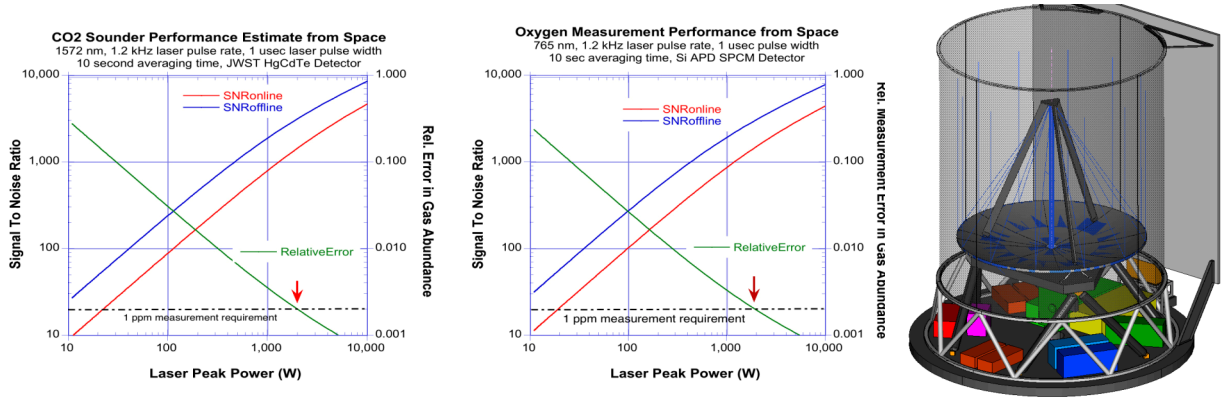

Figure 9 – Space lidar performance scaling and a lidar configuration for a 500 km orbit altitude. *Left* – Calculations for the CO_2 measurement SNR and relative error in column abundance vs laser peak power, for an assumed 1 usec laser pulse width, 10 sec of averaging time, based on receiver using a 1.5 m receiver diameter telescope and cooled HgCdTe APD detector. About 3 mJ/pulse is required, allowing for 3 dB margin. Similar performance can be achieved from a 450 km orbit with a NIR photomultiplier detector for the CO_2 measurement. *Middle* – A similar calculation for the O_2 measurement, assuming the receiver uses Si SPCM detectors, showing about the same energy is required with 3 dB margin. *Right* – The results of the initial space lidar study, showing a possible lidar configuration. Some elements shown are the 1.5 m receiver telescope, the radiator panel on the right, and most components mounted under the telescope's primary mirror.

The instrument size is determined by the 1.5 m receiver telescope and the size of the thermal radiator. The instrument power consumption is between 600 and 900W depending on the CO_2 detector choice and its sensitivity. An initial mass estimate was about 400 kg, and the uncompressed data rate was < 2 Mbits/sec. The primary thermal sources were the laser amplifier stages. The instrument's volume and mass fit comfortably within the capabilities of medium-sized rocket assuming a nominal spacecraft. Although more work is needed based using better-defined measurement requirements and lidar components, the studies found no major space instrument design concerns.

10. SUMMARY

We have developed a technique and demonstrated airborne measurements of CO_2 absorption and column abundance using a pulsed direct detection lidar based on the IPDA technique. The lidar operates by stepping its laser wavelength across a CO_2 line near 1572 nm. For space 8 wavelengths are planned and the line scan frequency is 1 Khz. The direct detection receiver measures the time resolved backscatter and absorption line shape in the column to the surface. The time resolved measurement approach allows CO_2 column measurements through thin clouds.

We demonstrated airborne lidar measurements during summer 2009 during flights between 3-13 km altitudes. Measurements were made using the 1572.33 nm CO_2 line in flights over several locations and some through cirrus clouds. They showed clear absorption line shapes, which increased in optical depth with increasing aircraft altitude. The instrument's line shapes were estimated via a CO_2 line shape retrieval algorithm, which permitted solving and correcting for known instrument factors. The post-processed line shapes agreed well with ones calculated from in-situ measurements and radiosondes.

We have since made several improvements to the airborne lidar. We have improved the instrument's optical transmission, calibrations and receiver SNR. We have made additional flights on the NASA DC-8 during July 2010, to 13 km altitude, over various sites. We have also demonstrated lidar measurements of O2 column absorption over horizontal paths, and in July 2010 we demonstrated airborne O2 column absorption measurements. Those measurements are being analyzed and will be reported in the future. This work shows progress with this candidate approach for the ASCENDS mission. However to meet the ASCENDS mission goals, further analysis of the measurement requirements, and improvements in calibration, precision, airborne stability, readout rate and laser power scaling are needed. These are being addressed in ongoing work.

11. ACKNOWLEDGEMENTS

We are grateful for the support of the NASA Earth Science Technology Office's Advanced Instrument Technology and Instrument Incubator Programs, the NASA Ascends Definition Program, and the Goddard IRAD program. We appreciate the collaboration with James Demers, Alan Mickleright and Steven Hughell of NASA Glenn, and the in-situ atmospheric measurements from Susan Kooi of NASA LaRC. We greatly appreciate the valuable work of other members of the Goddard CO_2 Sounder team.

REFERENCES

[1] Tans, P. P, Fung, I. Y., and Takahashi, T. "Observational constraints on the global atmospheric CO_2 budget," *Science* 247, pages 1431-1438 (1990).

[2] Fan, S., M. Gloor, J. Mahlman, S. Pacala, J. Sarmiento, T. Takahashi, P. Tans. "A large terrestrial carbon sink in North America implied by atmospheric and oceanic carbon dioxide data and models", *Science* 282: 442-446 (1998).

[3] Kuang, Z., Margolis, J., Toon, G., Crisp D., and Yung, Y., "Spaceborne measurements of atmospheric CO_2 by high-resolution NIR spectrometry of reflected sunlight: An introductory study," *Geophys. Res. Let.* 29(15), 1716, doi:10.1029/2001GL014298 (2002).

[4] O'Brien D. M. and Rayner, P. J., "Global observations of carbon budget 2, CO_2 concentrations from differential absorption of reflected sunlight in the 1.61 um band of CO_2," *J. Geophys. Res*. 107, 4354, doi:10.1029/2001JD000617 (2002).

[5] Dufour E. and Breon, F. M. "Spaceborne estimate of atmospheric CO_2 column by use of the differential absorption method: error analysis," *Appl. Opt.* 42, pages 3595-3609 (2003).

[6] Yokota, T., Oguma, H. , Morino, I. , Higurashi, A. , Aoki, T. and Inoue, G.. "Test measurements by a BBM of the nadir-looking SWIR FTS aboard GOSAT to monitor CO_2 column density from space," *Proc. SPIE* 5652, 182, DOI:10.1117/12.578497 (2004).

[7] Mao, J. and Kawa, S. R., "Sensitivity Study for Space-based Measurement of Atmospheric Total Column Carbon Dioxide by Reflected Sunlight," *Applied Optics*, **43**, 914-927 (2004).

[8] Aben, I., Hasekamp, O. and Hartmann, W., "Uncertainties in the space-based measurements of CO_2 columns due to scattering in the Earth's atmosphere," *J. Quant. Spectrosc. Radiat. Transfer,* **104**, 450-459 (2007).

[9] Uchino, O. and co-authors., "Initial Validation of GOSAT Standard Products, the 8th International Carbon Conference," Jena, Germany, September 13-19 (2009).

[10] United States National Research Council, "Earth Science and Applications from Space: National Imperatives for the Next Decade and Beyond," Available from http://www.nap.edu/. (2007).

[11] NASA ASCENDS Mission Science Definition and Planning Workshop Report, Available from: http://cce.nasa.gov/ascends/12-30-08%20ASCENDS_Workshop_Report%20clean.pdf (2008).

[12] ESA A-SCOPE Mission Assessment report, Available from http://esamultimedia.esa.int/docs/SP1313-1_ASCOPE.pdf (2008).

[13] Durand, Y., Caron, J., Bensi, P., Ingmann, P., Bézy, J., and Meynart, " A-SCOPE: Concepts for an ESA mission to measure CO_2 from space with a lidar," *Proceedings of the 8th International Symposium on Tropospheric Profiling, ISBN 978-90-6960-233-2 (2009)*.

[14] Ehret, G., Kiemle, C., Wirth, M., Amediek, A., Fix, A., and Houweling, S. "Space-borne remote sensing of CO_2, CH_4, and N_2O by integrated path differential absorption lidar: A sensitivity analysis," *Appl. Phys. B* ***90***, 593–608, DOI: 10.1007/s00340-007-2892-3 (2008).

[15] Caron, J. and Durand, Y., "Operating wavelengths optimization for a spaceborne lidar measuring atmospheric CO_2," *Applied Optics* 48, pages 5413-5422 (2009).

[16] Abshire, J. B., Riris, H., Allan, G. R., Weaver, C. J., Mao, J., Sun, X., Hasselbrack, W. E., Kawa, S. R. and Biraud, S., "Pulsed airborne lidar measurements of atmospheric CO_2 column absorption." *Tellus B*, no. doi: 10.1111/j.1600-0889.2010.00502.x (2010).

[17] Krainak, M.A, Andrews, A. E., Allan, G. R., Burris, J. F., Riris, H. , Sun, X., and Abshire, J. B., "Measurements of atmospheric CO_2 over a horizontal path using a tunable-diode-laser and erbium-fiber-amplifier at 1572 nm," in *Conference on Lasers and Electro-Optics, Technical Digest*, Optical Society of America, paper CTuX4, pages 878-881. ISBN: 1-55752-748-2 (2003).

[18] Riris, H., Abshire, J., Allan, G., Burris, J., Chen, J., Kawa, S., Mao, J., Krainak, M., Stephen, M., Sun, X., Wilson, E., "A laser sounder for measuring atmospheric trace gases from space," *Proc. of SPIE* Vol. 6750, 67500U doi: 10.1117/12.737607 (2007).

[19] Abshire, J. B., Riris, H., Sun, X., Krainak, M., Kawa, S., Mao, J., and Burris, J., "Lidar Approach for Measuring the CO_2 Concentrations in the Troposphere from Space," in *Proceedings of 2007 Conference on Lasers and Electro-Optics (CLEO-2007),* Optical Society of America, Paper CThII5, ISBN: 978-1-55752-834-6 (2007).

[20] Stephen, M., Krainak, M., Riris H., and Allan, G. R., "Narrowband, tunable, frequency-doubled, erbium-doped fiber-amplified transmitter," *Optics Letters*, Vol. 32, No. 15 pages 2073-6 (2007).

[21] Stephen, M.A., Mao, J., Abshire, J. B., Kawa, S.R., Sun X., Krainak, M.A., "Oxygen Spectroscopy Laser Sounding Instrument for Remote Sensing of Atmospheric Pressure," *IEEE Aerospace Conference*, pages 1-6, doi: 10.1109/AERO.2008.4526388 (2008).

[22] Measures, R., *Laser Remote Sensing: Fundamentals and Applications*, Krieger Publishing, New York (1992).

[23] Mao, J., Kawa, S. R., Abshire, J. B. and Riris, H., "Sensitivity Studies for a Space-based CO_2 Laser Sounder," *Eos Trans. AGU*, 88(52), Fall Meet. Suppl. Abstract A13D-1500(2007).

[24] Weitkamp, C., *Lidar: Range Resolved Optical Remote Sensing of the Atmosphere,* Springer, Berlin, Heidelberg, New York. (2005).

[25] Allan G. R., Riris, H., Abshire J. B., Sun X., Wilson E., Burris J.F., and Krainak, M.A., "Laser sounder for active remote sensing measurements of CO_2 concentrations," *Proceedings of 2008 IEEE Aerospace Conference*, pages 1534-1540, DOI: 10.1109/AERO.2008.4526387 (2008).

[26] NASA-Glenn Lear-25. Available from: http://www.grc.nasa.gov/WWW/AircraftOps/Learjet.html (2010).

[27] Abshire, J. B., Riris, H., Allan G.R., Weaver, C., Hasselbrack, W. and Sun, X., "Pulsed Airborne Lidar measurements of Atmospheric CO_2 Column Absorption and Line Shapes from 3-13 km altitudes," *Research Abstracts Vol. 12, EGU2010-7060*, 2010 EGU General Assembly (2010).

[28] Y. Choi, S.Vay, K. Vadevu, A. Soja, J. Woo, S. Nolf, G. Sachse, et. al., "Characteristics of the atmospheric CO_2 signal as observed over the conterminous United States during INTEX-NA", Journal of Geophysical Research, 113, D07301, (2008).

[29] S. Vay, J. Woo, B. Anderson, et al., " Influence of regional-scale anthropogenic emissions on CO_2 distributions over the western North Pacific", *Journal of Geophysical Research-Atmospheres*, 108 (2003).

[30] Rodgers, C., *Inverse Methods for Atmospheric Soundings, Theory and Practice,* Series on Atmospheric, Oceanic and Planetary Physics, vol. 2, World Scientific, page 238. (2000).

[31] X. Sun and J.B Abshire, "Receiver Performance Analysis of a Photon Counting Laser Sounder for Measuring Atmosphere CO_2 Concentration," *ILRC-25 Conference Proceedings,* St. Petersburg Russia (2010).

[32] A. Amediek et al., "Backscatter and Column Height Estimates from a pulsed airborne CO_2 Lidar*,"ILRC-25 Conference Proceedings*, St. Petersburg Russia (2010).